An Integrated HOCl-Producing E-Scaffold Is Active against Monomicrobial and Polymicrobial Biofilms

Laure Flurin,[a] Yash S. Raval,[a] Abdelrhman Mohamed,[c] Kerryl E. Greenwood-Quaintance,[a] Edison J. Cano,[b] Haluk Beyenal,[c] Robin Patel[a,b]

[a]Division of Clinical Microbiology, Mayo Clinic, Rochester, Minnesota, USA
[b]Division of Infectious Diseases, Mayo Clinic, Rochester, Minnesota, USA
[c]The Gene and Linda Voiland School of Chemical Engineering and Bioengineering, Washington State University, Pullman, Washington, USA

ABSTRACT Oxidizing agents like hypochlorous acid (HOCl) have antimicrobial activity. We developed an integrated electrochemical scaffold, or e-scaffold, that delivers a continuous low dose of HOCl aimed at targeting microbial biofilms without exceeding concentrations toxic to humans as a prototype of a device being developed to treat wound infections in humans. In this work, we tested the device against 33 isolates of bacteria (including isolates with acquired antibiotic resistance) grown as *in vitro* biofilms alongside 12 combinations of dual-species *in vitro* biofilms. Biofilms were grown on the bottoms of 12-well plates for 24 h. An integrated e-scaffold was placed atop each biofilm and polarized at 1.5 V for 1, 2, or 4 h. HOCl was produced electrochemically by oxidizing chloride ions (Cl^-) in solution to chlorine (Cl_2); dissolved Cl_2 spontaneously dissociates in water to produce HOCl. The cumulative concentration of HOCl produced at the working electrode in each well was estimated to be 7.89, 13.46, and 29.50 mM after 1, 2, and 4 h of polarization, respectively. Four hours of polarization caused an average reduction of 6.13 $\log_{10}$ CFU/cm^2 (± 1.99 $\log_{10}$ CFU/cm^2) of viable cell counts of monospecies biofilms and 5.53 $\log_{10}$ CFU/cm^2 (± 2.31 $\log_{10}$ CFU/cm^2) for the 12 dual-species biofilms studied. The described integrated e-scaffold reduces viable bacterial cell counts in biofilms formed by an array of antibiotic-susceptible and -resistant bacteria alone and in combination.

KEYWORDS hypochlorous acid, biofilm, treatment, wound infections, electrochemistry

Infections related to bacteria in biofilms are more difficult to treat than those caused by planktonic forms of microorganisms because of the poor activity of most conventional antibiotics against biofilm and biofilm tolerance to host immunity (1). Biofilms consist of a dense aggregate of bacteria or fungi enclosed in a self-produced matrix composed of extracellular polymeric substance (EPS). Within biofilms, there is limited diffusion of nutrients, oxygen, and some antimicrobial agents, and resident microbial cells grow slowly (2). Many cells assume such a low growth rate that they are referred to as persisters or dormant cells, contributing to antibiotic tolerance and relapses in biofilm-related infections (3). Cells in biofilms can survive in spite of antibiotic therapy, especially in the face of antibiotics that rely on growth, assuming an actively growing phenotype when antibiotics are removed, thereafter recolonizing infection sites (2). Besides antibiotic tolerance, another challenge in biofilm treatment is acquired antibiotic resistance, associated with mutations or horizontal gene transfer, which can be enhanced in biofilms (4). Biofilms may form on either inert surfaces (as in the case of device-related infections) or biotic surfaces, including human tissues, such as on wounds (5). As a result, bacteria in biofilm-associated wound infections show high levels of tolerance to conventional antibiotics (6–8), and low antibiotic concentrations may reach bacterial cells in wounds, facilitating the selection of acquired antimicrobial resistance (2, 9).

Address correspondence to Robin Patel, patel.robin@mayo.edu.

The microbiology of chronic wound infections can be diverse and is dependent on the location and type of wound (10). Chronic wound infections are often polymicrobial, composed of mixed communities, including Gram-positive and -negative aerobic and facultatively anaerobic bacteria, anaerobic bacteria, and fungi (11–13); polymicrobial biofilms add complexity to treatment. Some studies have shown a negative impact of polymicrobial compared to monomicrobial wound infections on patient outcomes and wound healing (14).

Alternatives to antibiotic therapy are needed to treat wound biofilms. Topical agents like NaOCl (Dakin's solution) or povidone-iodine are often used and can lead to biofilm eradication. While they reduce wound biofilms, cytotoxicity may impair tissue healing (15). Thus, they are not recommended for treatment of chronic venous ulcers. Oxidizing agents like hypochlorous acid (HOCl) or hydrogen peroxide (H_2O_2), which are naturally produced intracellularly by neutrophils during the oxidative burst triggered by pathogen phagocytosis (15, 16), are used as wound cleansers (17). They are interesting considerations for biofilm treatment, especially because they directly target bacterial cells in a non-growth-dependent manner, making it theoretically possible to affect dormant cells. Moreover, HOCl has a broad spectrum of antibacterial activity (15) and may promote tissue healing (18, 19). HOCl penetrates bacterial cells, where it inhibits DNA synthesis and oxidizes thiol-containing proteins, alongside disrupting ATP production. However, when used as a solution, the active molecule does not persist over time, limiting activity; further, concentrations above 286 μM delivered at once are cytotoxic (15).

As a means of sustained delivery of HOCl, we are developing an electrochemical scaffold, or e-scaffold, that delivers a continuous low dose of HOCl aimed at targeting biofilms, without exceeding concentrations toxic to humans, as a prototype of a device that could ultimately be used to treat clinical infections, such as wound infections. Our e-scaffold is composed of three electrodes (counter, working, and reference) polarized at $+1.5$ $V_{Ag/AgCl}$. We previously showed an earlier version of the e-scaffold to be active against *Staphylococcus aureus*, *Pseudomonas aeruginosa*, *Acinetobacter baumannii*, and *Candida* biofilms *in vitro* (20, 21). The design of the e-scaffold has been improved since our previous work (20, 21) by integrating a reference electrode into the e-scaffold (a design we refer to as an integrated e-scaffold), creating a unit that can ultimately be further adapted for *in vivo* use, for example, on wound surfaces. In our previous work, we used an external electrode that was large and impractical for *in vivo* application. Moreover, our e-scaffold was not tested against mixed-culture biofilms, which is important for its clinical applications.

In this work, we tested the spectrum of activity of the newly designed integrated e-scaffold. Specifically, we tested the integrated e-scaffold *in vitro* against 33 isolates of bacteria and 12 combinations of dual-species biofilms at three endpoints, 1, 2, and 4 h. Dual-species combinations tested in this study were selected according to their frequency in the literature. The microbiology of wound infections differs by wound type, chronicity, and geographic region (e.g., temperate versus tropical countries). In chronic wound infections, such as infected pressure ulcers, more than 50% of infections are polymicrobial, with the most common pathogens being Enterobacterales, *S. aureus*, and nonfermenting Gram-negative bacteria, such as *P. aeruginosa* and *A. baumannii* (12, 22–24). In the case of diabetic foot infections (6, 25–28), *P. aeruginosa*, *Enterococcus* species, *S. aureus*, and *Escherichia coli* are commonly found in polymicrobial cultures. Among anaerobic/aerotolerant bacteria, *Bacteroides fragilis* is the most frequently found microorganism in polymicrobial wound infections, where it is often associated with *S. aureus* and/or Gram-negative bacteria (29–31). In addition to selection of combinations based on a review of the literature, we chose combinations of the most challenging pathogens in terms of clinical severity and treatment challenge. For example, multidrug-resistant wound infections associated with *A. baumannii* are devastating in traumatic injuries during wars in the Middle East (32). Enterococcal wound infections are often polymicrobial and associated with high severity (33). *P. aeruginosa* and *S. aureus* are a common dual-species combination in

infection in wounds, often associated with high virulence (34). In addition, we studied antibiotic-resistant isolates that represent a challenge in clinical practice, including methicillin-resistant *S. aureus* (MRSA), vancomycin-resistant enterococci (VRE), multidrug-resistant (MDR) *P. aeruginosa*, and carbapenem-resistant *E. coli*, *Klebsiella pneumoniae*, and *A. baumannii* (35).

The objectives of this study were to (i) improve our previous e-scaffold to include an integrated reference electrode and (ii) test its spectrum of antibiofilm activity, including that in the polymicrobial scenario.

RESULTS

**Estimation of the HOCl concentration produced by the integrated e-scaffold.** The current going through each integrated e-scaffold was measured and reported for each replicate experiment at each endpoint (Fig. 1 and Table 1). Means of the current measured after 1, 2, and 4 h of polarization were 1.48, 1.26, and 1.38 mA, respectively. Based on these measurements, the cumulative concentration of HOCl produced at the working electrode in one well was estimated to be 7.89 mM after 1 h of polarization, 13.46 mM after 2 h of polarization, and 29.50 mM after 4 h of polarization.

Treatment of monospecies biofilms. Before treatment, the average viable biofilm cell quantity was 7.8 $\log_{10}$ CFU/cm^2 (± 0.46 $\log_{10}$ CFU/cm^2) (Fig. 2). Four hours of polarization caused an average reduction of viable cells in monospecies biofilms of 6.13 $\log_{10}$ CFU/cm^2 (± 1.99 $\log_{10}$ CFU/cm^2). Each monospecies biofilm had a mean reduction of viable cells at 4 h of treatment of >3 $\log_{10}$ CFU/cm^2, except *S. epidermidis* Xen 43, which had a mean reduction of 2.37 $\log_{10}$ CFU/cm^2. There was variability in the time frame of effect, with differences noted between aerobic/facultatively anaerobic Gram-positive and Gram-negative bacteria. For example, viable cell measurements of all Gram-negative bacteria tested were reduced below the limit of detection at 4 h of polarization, with a mean reduction for this group of 7.81 $\log_{10}$ CFU/cm^2 (± 0.48 $\log_{10}$ CFU/cm^2). On the other hand, for aerobic/facultatively anaerobic Gram-positive isolates, a reduction to below the limit of detection at 4 h was only observed for *S. aureus* IDRL-8661, *Enterococcus faecium* IDRL-11790, and *S. mutans* IDRL-7131. The mean biofilm viable cell count reduction for the aerobic/facultatively anaerobic Gram-positive bacteria tested was 5.23 $\log_{10}$ CFU/cm^2 (± 1.84 $\log_{10}$ CFU/cm^2) at 4 h. With an average viable cell reduction of 3.67 $\log_{10}$ CFU/cm^2 (± 0.54 $\log_{10}$ CFU/cm^2) at 4 h, anaerobic/aerotolerant isolates had significant but slightly lower reductions than aerobic/facultatively anaerobic isolates.

Dual-species biofilms. Of the 12 polymicrobial biofilms studied, 11 showed a mean reduction of more than 3 $\log_{10}$ CFU/cm^2 in viable cell counts after 4 h of treatment (Fig. 3). Polarization generated a mean viable cell count reduction of 5.53 $\log_{10}$ CFU/cm^2 (± 2.31 $\log_{10}$ CFU/cm^2) among the 12 combinations at 4 h. The only isolate that did not respond in coculture was *E. faecium* IDRL-11790. It was the only isolate that had a mean viable cell count reduction after 4 h of treatment of less than 3 $\log_{10}$ CFU/cm^2. In comparison, in a monospecies biofilm, viable counts of *E. faecium* IDRL-11790 were reduced below the limit of detection at 4 h. After treatment, cell quantities of *E. faecium* IDRL-11790 were higher than when in monospecies biofilms or when cocultured with *P. aeruginosa* IDRL-11442 ($P = 0.0078$), *S. aureus* IDRL-6169 ($P = 0.0039$), or *E. coli* IDRL-10366 ($P = 0.308$) (see Fig. S1 in the supplemental material). In contrast, viable counts of *S. aureus* IDRL-6169 biofilms were more reduced after 4 h of treatment in coculture with *P. aeruginosa* IDRL-11442 ($P = 0.0039$) or *S. epidermidis* ATCC 35984 ($P = 0.0039$) than when grown alone. For the other combinations of bacteria studied, there were no obvious differences in responses alone or in dual-species biofilms.

DISCUSSION

Here, we describe a device referred to as an integrated e-scaffold, a more advanced version of our previously described e-scaffold (20, 21). The integrated e-scaffold described here delivers HOCl continuously. Our ultimate goal is to advance this device to an electrochemical bandage to treat wound infections.
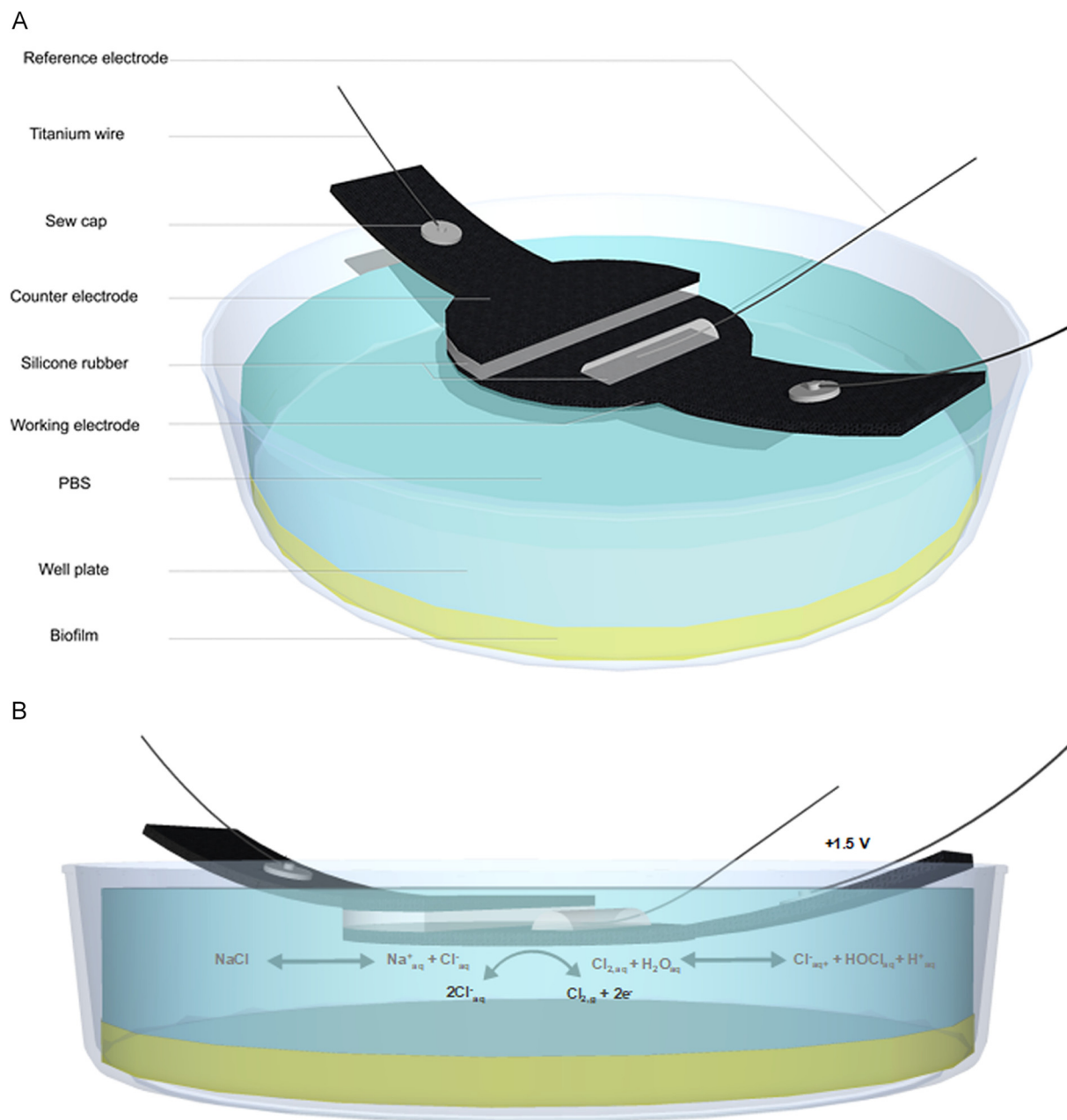
FIG 1 Illustration of the integrated e-scaffold. (a) Schematic illustration of the experimental setup. Each device was submerged in a well of a 12-well plate containing PBS composed of 32 mmol liter^{-1} dipotassium phosphate (K_2HPO_4), 18 mmol liter^{-1} monopotassium phosphate (KH_2PO_4), and 0.9% (wt/vol) sodium chloride (NaCl), pH 7.0 (b) Chloride ions supplied by the dissociation of NaCl oxidized to chlorine at the working electrode (+1.5 $V_{Ag/AgCl}$).

The cumulative concentration of HOCl produced during treatment was estimated based on current. The average estimated cumulative amount of HOCl produced in this experiment approximated that previously determined by our group using an older e-scaffold version that had a separate large reference electrode (21).

TABLE 1 Estimated HOCl concentrations produced

Treatment exposure (h)	Avg ± SD current (mA)	Estimated avg total HOCl concn (mM)
1	1.48 ± 1.07	7.89
2	1.26 ± 0.78	13.46
4	1.38 ± 0.73	29.50
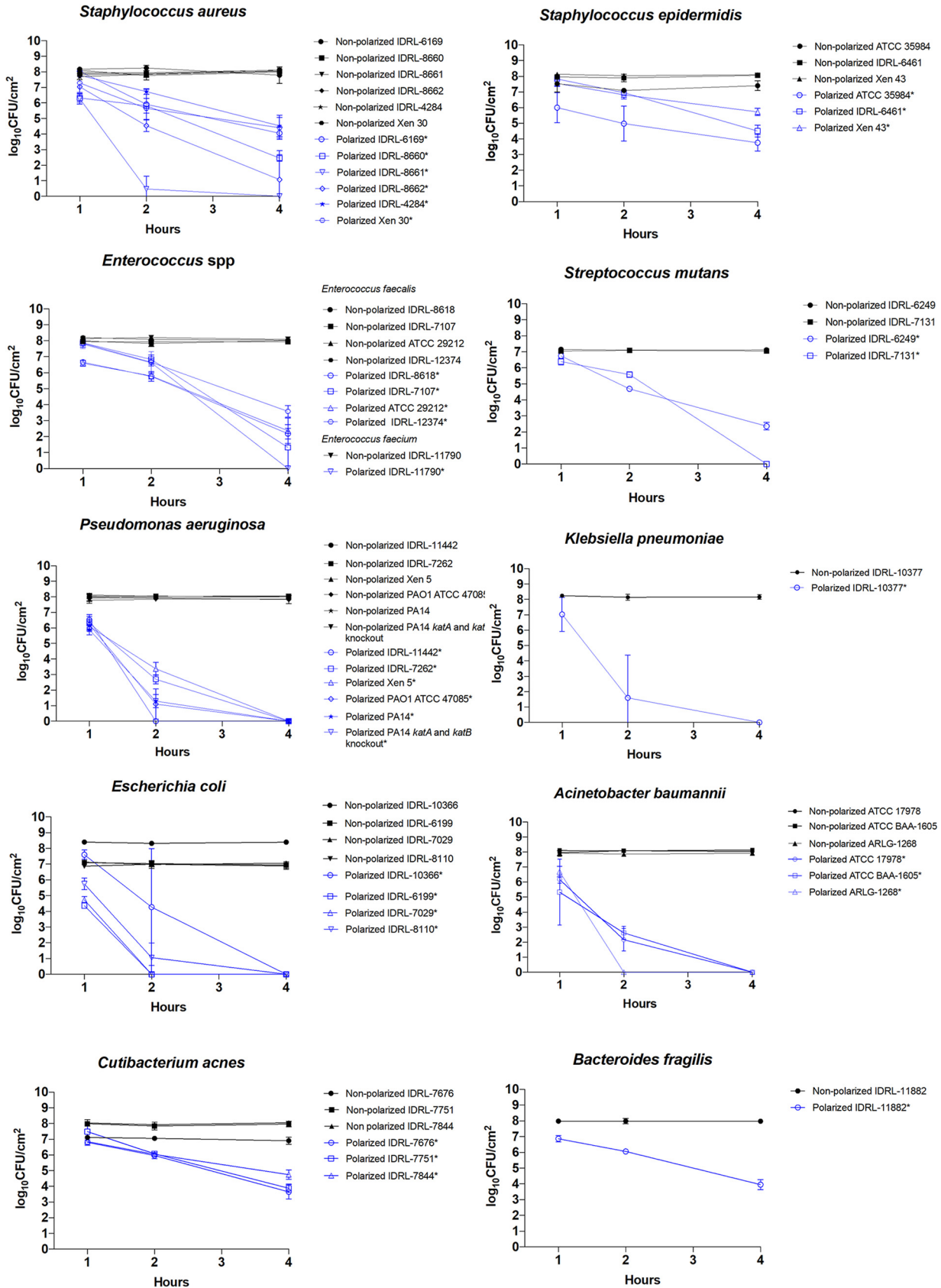
FIG 2 Results of treatment of monospecies biofilms. Results are displayed at 1, 2, and 4 h of treatment. Data are plotted as means, and error bars represent standard deviations. Statistical significance ($P < 0.05$) is indicated by an asterisk in the legends next to each isolates name.
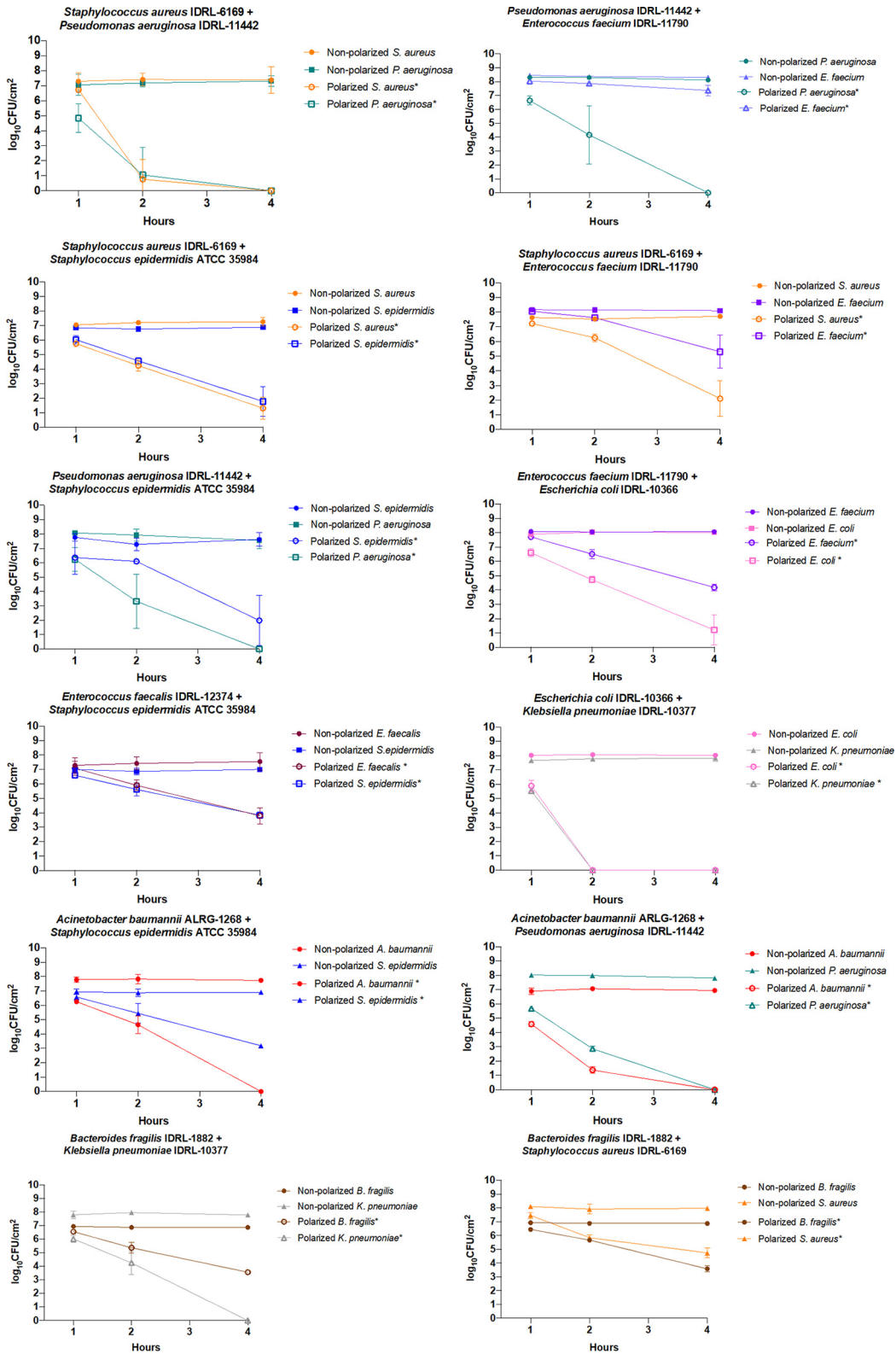
FIG 3 Results of treatment of dual-species biofilms. Results are displayed at 1, 2, and 4 h of treatment. Data are plotted as means, and error bars represent standard deviations. Results of statistical analysis reported are a comparison between one isolate's nonpolarized and polarized cell quantity. Statistical significance ($P < 0.05$) is indicated by an asterisk in the legends next to each species name.

Viable cell counts from *in vitro* biofilms of one and two species formed by a wide selection of bacteria were reduced by the HOCl-generating integrated e-scaffold. We found activity against *P. aeruginosa*, *A. baumannii*, and *S. aureus* similar to that in our previously published work with our older (nonintegrated) e-scaffold design (20, 21). We also expanded the tested species to include *S. epidermidis*, *E. faecalis*, *E. faecium*, *S. mutans*, *E. coli*, *K. pneumoniae*, *B. fragilis*, and *Cutibacterium acnes*. Overall, the effect was faster for some organisms, especially the Gram-negative aerobic/facultatively anaerobic group, which showed reductions to below the limit of detection of the assay used (10 CFU/ml) at 4 h.

We hypothesize that thickness of the cell wall plays a role in the differences observed between aerobic/facultatively anaerobic Gram-negative and Gram-positive species in our experiments. HOCl must pass through the cell envelope to exhibit antimicrobial activity. Because HOCl is electrically neutral, it likely enters cells by passive diffusion. Inside cells, it alters the energy transport system of the cell, leading to rapid ATP hydrolysis (36–38). Gram-positive bacteria have a thicker cell wall ($\sim$20 to 80 nm) than Gram-negative bacteria (<10 nm) (39). Therefore, passive diffusion through Gram-negative bacterial cell walls could be quicker than through Gram-positive bacterial cell walls. Differences between Gram-positive and -negative cells will be further examined in our future work, focused on the mechanism of action of HOCl.

Among the four isolates of anaerobic/aerotolerant bacteria tested, reduction in viable cells was 3.67 $\log_{10}$ CFU/cm^2 at 4 h. Anaerobic bacteria can be associated with delayed wound healing (40, 41). Longer treatment periods may be needed to address wound infections involving anaerobes compared to those limited to aerobes.

Differences between isolates could relate to different structures of associated biofilms, biofilm matrices, and penetration of HOCl into biofilms. Differences between dual- and monospecies biofilms possibly could be explained by isolates' interactions with each other. For example, *P. aeruginosa* wound infections are often severe and may be harder to treat than infections caused by other bacterial species, in part due to the intrinsic and acquired antibiotic resistance in this species. The integrated e-scaffold displayed rapid and consistent activity against all *P. aeruginosa* isolates tested in mono- and dual-species experiments. As shown in a wound model study by DeLeon et al., dual-species biofilms comprised of *P. aeruginosa* and *S. aureus* display higher tolerance to antibiotics than monospecies biofilms of the same species (42). Our results show that when treated together, *S. aureus* and *P. aeruginosa* were killed faster than in monospecies biofilms. Interestingly, when *S. aureus* and *P. aeruginosa* are grown together planktonically, *P. aeruginosa* overcomes *S. aureus* by killing it through protease LasA (43), 2-*n*-heptyl-4-hydroxyquinoline N-oxide (HQNO), and/or phenazine pyocyanin production (44). In a study of chloroxylenol treatment of mixed biofilms composed of *S. aureus* and *P. aeruginosa*, when exposed to chloroxylenol, the *P. aeruginosa* exoproduct HQNO increased *S. aureus* biofilm and planktonic susceptibility to chloroxylenol by increasing *S. aureus* membrane's fluidity (45). Further studies should investigate the role of HQNO in the context of HOCl treatment.

The involvement of *Enterococcus* species in polymicrobial infections is beginning to be studied from clinical and microbiological standpoints (46–48). In the particular case of combat wound infections, enterococci are often associated with polymicrobial infections involving *P. aeruginosa*, *E. coli*, *K. pneumoniae*, *A. baumannii*, and/or *S. aureus*, and such polymicrobial wound infections can be associated with higher intensive care unit admission rates and longer durations of hospitalization than monomicrobial wound infections (33). In a study of *S. aureus* phage therapy of dual-species biofilms made of *S. aureus* and *E. faecium*, treatment increased viable cell quantities of *E. faecium* (49). Additional studies are needed to assess interactions between *E. faecium* and *S. aureus*, *P. aeruginosa*, or *E. coli*.

Unexpected results were found with the combination of *S. aureus* and *S. epidermidis*. When treated alone, we found a viable cell count reduction of 3.73 $\log_{10}$ CFU/cm^2 for *S. aureus* IDRL-6169. However, when grown and treated as a dual-species biofilm

with *S. epidermidis* ATCC 35984, the reduction at 4 h was 5.96 $\log_{10}$ CFU/cm². Several studies have focused on understanding interactions between *S. aureus* and *S. epidermidis* in biofilms; *S. epidermidis*, through serine protease Esp, has been shown to inhibit *S. aureus* biofilm formation (50, 51).

Variability in HOCl treatment effects has been shown *in vitro* with stabilized HOCl solution (15). In one study, the minimum bactericidal concentration of HOCl tested for 60 min was variable and high for *Aspergillus niger*, vancomycin-resistant *E. faecium*, *Candida albicans*, *Staphylococcus hominis*, and *Micrococcus luteus*. In *in vitro* time-kill studies, *Streptococcus pyogenes* required longer than 10 min to be killed, while *P. aeruginosa* and most other species were eliminated after less than 1 min.

Overall, we demonstrated that our integrated e-scaffold reduced the viable cell counts of a wide array of biofilms, with some variability between species and in mixed-species biofilms. Given the variability of activity for certain species or strains, varying concentrations of HOCl and/or varying exposure times to the integrated e-scaffold could be considered, especially in future *in vivo* studies. Individualized treatment regimens could possibly be designed by performing *in vitro* time-kill tests (such as those described here). That way, it may be possible to find a balance between antimicrobial activity and potential toxicity by, for example, adapting the time of exposure and the concentration of HOCl delivered directly to the organism(s) targeted.

Our study has several limitations. First, the *in vitro* assay does not necessarily represent the conditions, shapes, and sizes of human wounds; since the device is made with flexible carbon fabric, it can easily be adapted to different shapes and sizes of wounds. Second, the assay was performed in liquid rather than a dry wound model. However, it is expected that, *in vivo*, NaCl will be supplied by biological fluids such as wound exudate and blood. Another limitation is that we did not directly measure HOCl. However, in our previous work (21), we determined that 5 μM HOCl was produced at a potential of $+1.5$ $V_{Ag/AgCl}$ during 10 min. This value is below the reported toxic concentration of HOCl (286 μM). In this study, estimations of HOCl concentrations were calculated considering chloride oxidation to be the dominant working electron reaction (i.e., 100% of electrons going toward chloride oxidation and HOCl production). Therefore, 29.5 mM is the upper limit of the cumulative HOCl that the device can deliver in 4 h. We note that HOCl is unstable and sensitive to UV light and temperature (52). Our experiment was set under conditions that would mimic *in vivo* experiments, that is, at 25°C and with no UV filter. Therefore, it is probable that HOCl was autodegraded or consumed as it is produced; in this way, we do not expect the HOCl concentration to reach above 286 μM. Toxicity was not, however, assessed here. It was evaluated in our previous work, where HOCl-producing e-scaffolds were applied to explanted pig ears; after 3 h of exposure, there were no pathological findings, and there were no findings of cytotoxicity after 48 h (20, 21). In another study, after 6 and 24 h of exposure of noninfected porcine explants, histopathologic analysis highlighted some tissue damage but cell viability was not changed (20). Whether or not resistance to the effects reported with prolonged applications of HOCl will emerge is unknown; HOCl resistance was previously described in *E. coli* and *Salmonella* species in the food industry (53, 54).

In conclusion, the described integrated e-scaffold decreases viable cell counts in biofilms formed by a wide selection of antibiotic-susceptible and -resistant bacteria, including those present in dual-species biofilms.

MATERIALS AND METHODS

Integrated e-scaffold. The integrated e-scaffold is shown in Fig. 1a. The counter and working electrodes are made of a conductive carbon fabric, Panex 30 PW-06 (Zoltek Companies Inc., St. Louis, MO), custom cut in a semilunar and lunar shape, respectively. Before assembly, the carbon fabric was treated in 1 M HOCl overnight and washed and dried to improve wettability. Counter and working electrodes were glued atop one another using a thin layer of silicon rubber, ensuring that their surfaces were not in direct contact with one another. The reference electrode was a silver-silver chloride wire affixed using silicone rubber on top of the surface of the working electrode. AgCl was deposited on a silver wire to make the reference electrode, using procedures described in reference 55. Nylon sew snaps (item number 85; Dritz, Spartanburg, SC) were used to press titanium wires (catalog number RW0524; TEMCo) onto

TABLE 2 Bacteria studied, strain number, source, and antibiotic resistance

Species	Isolate	Source	Resistance	Details
Staphylococcus aureus	IDRL-8660	Henry Chambers	Methicillin	USA 100
S. aureus	IDRL-8661	Henry Chambers	Methicillin	USA 200
S. aureus	IDRL-8662	Henry Chambers	Methicillin	USA 300
S. aureus	IDRL-6169	Prosthetic hip infection	Methicillin	
S. aureus	Xen30	Caliper Life Sciences	Methicillin	
S. aureus	IDRL-4284	Unknown		
Staphylococcus epidermidis	ATCC 35984	Catheter infection	Methicillin	
S. epidermidis	IDRL-6461	Prosthetic knee infection		
S. epidermidis	Xen 43	Caliper Life Sciences		
Enterococcus faecalis	ATCC 29212	Urinary tract infection		
E. faecalis	IDRL-12374	Prosthetic hip infection	Vancomycin	
E. faecalis	IDRL-7107	Prosthetic knee infection		
E. faecalis	IDRL8618	Prosthetic hip infection		
Enterococcus faecium	IDRL-11790	Abscess	Vancomycin	
Streptococcus mutans	IDRL 7131	Prosthetic knee infection		
S. mutans	IDRL-6249	Bacteremia		
Escherichia coli	IDRL-10366	Clinical microbiology laboratory	Carbapenem	bla_{KPC} positive
E. coli	IDRL-7029	Prosthetic hip infection		
E. coli	IDRL-6199	Prosthetic knee infection		
E. coli	IDRL-8110	Bacteremia		
Pseudomonas aeruginosa	IDRL-7262	Prosthetic hip infection		
P. aeruginosa	Xen 5	Caliper Life Sciences Bacteremia		
P. aeruginosa	PAO1 ATCC 47085	Wound infection		
P. aeruginosa	PA14	Daniel Hassett		
P. aeruginosa	PA14 *katA* and *katB* knockout	Daniel Hassett		
P. aeruginosa	IDRL-11442	Groin wound infection	Carbapenem	Colistin susceptible
Acinetobacter baumannii	ATCC 17978	Meningitis		
A. baumannii	ATCC BAA-1605	Respiratory tract infection	Imipenem	
A. baumannii	ALRG-1268	Wound infection	Imipenem	Colistin susceptible
Klebsiella pneumoniae	IDRL-10377	Clinical microbiology laboratory	Carbapenem	bla_{KPC} positive
Bacteroides fragilis	IDRL-11882	Prosthetic knee infection		
Cutibacterium acnes	IDRL-7676	Prosthetic shoulder infection		
C. acnes	IDRL-7751	Spine implant-associated infection		
C. acnes	IDRL-7844	Spine implant-associated infection		

the conductive fabric, establishing electrical connections for working and counter electrodes. E-scaffolds were steam sterilized in an autoclave (Fisherbrand SterilElite Tabletop Autoclaves) at 121°C for 20 min. Working, counter, and reference electrodes were then connected to a custom-built potentiostat through titanium wires, and the working electrode was positively polarized against the reference electrode at +1.5 $V_{Ag/AgCl}$ (56).

Selection of inoculum. Before starting experiments, we determined the inoculum needed to obtain a cell quantity of ~7 to 8 $\log_{10}$ CFU/cm² for each isolate studied in dual-species biofilms. First, the inoculum was determined for dual-species biofilms and then applied to monospecies biofilms. For dual-species biofilms, we started by determining the concentration of inoculum needed to achieve relatively equal amounts of each isolate in dual-species biofilms. To do so, we tested two inocula of each isolate to form dual-species biofilms (i.e., four combinations per dual-species biofilm). We quantified viable cells in biofilms and chose the concentration that resulted in a total bacterial amount of ~7.5 $\log_{10}$ CFU/cm², with a relatively equal distribution of each species. For most isolates, a starting inoculum of 1 µl of 10⁸ CFU/ml was chosen. For *P. aeruginosa* IDRL-11442, the starting inoculum was lowered, since it otherwise overgrew its partner isolate in biofilms; an inoculum of 1 µl of 10⁴ CFU/ml was selected for all *P. aeruginosa* isolates. For *S. epidermidis* ATCC 35984, we chose a higher volume of inoculum (2 µl) of a higher concentration (10⁹ CFU/ml); absent this, its cell quantity was lower than that of its partner isolate. These amounts were used for all *S. epidermidis* isolates tested. For *B. fragilis*, a 10-µl inoculum of a concentration of 3 × 10⁸ CFU/ml was needed. Volumes and concentrations used for each isolate to form dual-species biofilms were used for monospecies biofilms. As a result, for monospecies biofilms, we used a concentration of 1 µl of 1.5 × 10⁸ CFU/ml for most isolates except *P. aeruginosa*, *S. epidermidis* isolates, and anaerobic/aerotolerant species.

Biofilm *in vitro* assay. Bacteria studied are shown in Table 2. One colony was added to 5 ml of Trypticase soy broth (TSB) and incubated at 37°C on a shaker until reaching 1.5 × 10⁸ CFU/ml (10⁴ CFU/ml for *P. aeruginosa*). One microliter (2 µl for *S. epidermidis*) of the bacterial broth plus 1 ml of TSB was then inoculated into each well of a 12-well nontreated cell culture plate (product number 351143; Falcon) and incubated for 24 h at 37°C without shaking to allow biofilm formation on well bottoms. For anaerobic/aerotolerant species (*Cutibacterium acnes* and *B. fragilis*) and *Streptococcus mutans*, 1 colony

TABLE 3 Microorganism pairs studied as dual-species biofilms and selective agar plate

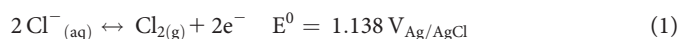| Pair	Selective agar plate
Staphylococcus aureus IDRL-6169 + *Pseudomonas aeruginosa* IDRL-11442	Colistin nalidixic acid (CNA) and eosin methylene blue (EMB) agar
S. aureus IDRL-6169 + *Staphylococcus epidermidis* ATCC 35984	Mannitol salt agar
S. aureus IDRL-6169 + *Enterococcus faecium* IDRL-11790	CHROMagar MRSA and CHROMagar VRE
P. aeruginosa IDRL-11442 + *E. faecium* IDRL-11790	CNA and EMB
P. aeruginosa IDRL-11442 + *S. epidermidis* ATCC 35984	CNA and EMB
Klebsiella pneumoniae IDRL-10377 + *Escherichia coli* IDRL-10366	CHROMagar Orientation agar
E. coli IDRL-10366 + *E. faecium* IDRL-11790	CNA and EMB
Enterococcus faecalis IDRL-12374 + *S. epidermidis* ATCC 35984	CHROMagar VRE and Mannitol salt agar
Acinetobacter baumannii ARLG-1268 + *S. epidermidis* ATCC 35984	CNA and EMB
A. baumannii ARLG-1268 + *P. aeruginosa* IDRL-11442	CHROMagar *P. aeruginosa* and CHROMagar *A. baumannii*
Bacteroides fragilis IDRL-11882 + *S. aureus* IDRL-6169	*Bacteroides fragilis* isolation agar and CHROMagar MRSA
B. fragilis IDRL-11882 + *Klebsiella pneumonaie* IDRL-10377	*Bacteroides fragilis* isolation agar and CHROMagar orientation

of bacteria was inoculated into 5 ml of brain heart infusion (BHI) broth supplemented with 1% glucose. *C. acnes* and *B. fragilis* were incubated in anaerobic jars and *S. mutans* in a 5% CO_2 atmosphere, all at 37°C, until the cultures reached 3×10^8 CFU/ml. Ten microliters of bacterial broth and 1 ml of BHI broth supplemented with 1% glucose then were inoculated into each well of a 12-well plate. Twelve-well plates containing *C. acnes* or *B. fragilis* were placed in anaerobic jars and incubated at 37°C for 2 days. Twelve-well plates containing *S. mutans* were incubated in a CO_2 incubator at 37°C for 2 days.

After incubation in the 12-well plates, TSB or BHI broth was removed and 3.5 ml of 1× sterile phosphate-buffered saline (PBS) was added to each well before application of an integrated e-scaffold.

Treatment. A sterile integrated e-scaffold was carefully placed atop each biofilm (control and treatment), as shown in Fig. 1b. The distance between the e-scaffold and the biofilm was kept as small as possible. Before polarization, cyclic voltammetry was applied from 0 $V_{Ag/AgCl}$ to +2.0 $V_{Ag/AgCl}$ to condition the integrated e-scaffold (scan rates, 100 mV/s and 10 mV/s). The integrated e-scaffold was polarized at +1.5 $V_{Ag/AgCl}$ for 1, 2, and 4 h. A negative control (nonpolarized integrated e-scaffold) was included for each endpoint. A sterilized TSB-filled well was used to verify the system was not contaminated for each run.

Biofilm quantification. After treatment, biofilms were scraped from the bottom and edges of each well plate and from each integrated e-scaffold's surface with sterile pipette tips, and the suspensions were combined, vortexed, and centrifuged at 5,000 rpm for 10 min. The cell pellet was resuspended in 1 ml of sterile saline and serial dilutions prepared: 100 μl of each dilution was spread-plated onto blood agar plates for monospecies biofilms or on selective and differential agars to differentiate species for dual-species biofilms (Table 3). Plates were incubated at 37°C for 48 h and CFU counted, with data reported as $\log_{10}$ CFU/cm^2. One hundred microliters of biofilm suspension was put in 5 ml of TSB and incubated for 48 h at 37°C in 5% CO_2 with shaking. If the broth was clear, the cell quantity was recorded as ≤10 CFU/ml (the limit of detection of the assay).

Estimation of HOCl concentration produced by the integrated e-scaffold. HOCl was produced electrochemically by oxidizing chloride ions (Cl$^-$) in solution to chlorine (Cl$_2$) (equation 1). Dissolved Cl$_2$ spontaneously dissociates in water to produce HOCl (equation 3). The cumulative HOCl concentration produced by the integrated e-scaffold was estimated using reaction stoichiometry (equations 1–3). The amount of electrons passing through the working electrode was calculated using current data collected by the potentiostat. Current data were integrated over time to calculate total charge delivered through the working electrode. The HOCl concentration was then estimated using reaction stoichiometry (1 mol HOCl: 2 mol e$^-$). The HOCl calculation was performed assuming that the anodic current was dominated by a chloride oxidation reaction (100% Faradaic efficiency). This method was used to estimate the total concentration of HOCl delivered to each well for 1-, 2-, and 4-h treatments.

$$2\,Cl^-_{(aq)} \leftrightarrow Cl_{2(g)} + 2e^- \quad E^0 = 1.138\,V_{Ag/AgCl} \tag{1}$$

$$Cl_{2(g)} \leftrightarrow Cl_{2(aq)} \tag{2}$$

$$Cl_{2(aq)} + H_2O \leftrightarrow Cl^-_{(aq)} + HOCl_{(aq)} + H^+_{(aq)} \tag{3}$$

Statistical analysis. Data were displayed as means with standard deviations, generated with GraphPad Prism version 8.0. Each data point corresponded to at least 3 replicates. Viable cell count reductions were calculated by comparing quantitative cultures of nonpolarized and polarized biofilms. Results, in numbers of CFU per square centimeter, were transformed into a logarithmic scale. A log reduction of 3 (i.e., 99.9%) was considered a meaningful reduction of viable bacteria (57). Comparisons between nonpolarized and polarized data were done using a Wilcoxon rank sum test. All tests were two-sided; *P* values of <0.05 were considered statistically significant.

REFERENCES

1. Hoiby N, Bjarnsholt T, Givskov M, Molin S, Ciofu O. 2010. Antibiotic resistance of bacterial biofilms. Int J Antimicrob Agents 35:322–332. https://doi.org/10.1016/j.ijantimicag.2009.12.011.
2. Hall CW, Mah TF. 2017. Molecular mechanisms of biofilm-based antibiotic resistance and tolerance in pathogenic bacteria. FEMS Microbiol Rev 41:276–301. https://doi.org/10.1093/femsre/fux010.
3. Conlon BP, Rowe SE, Lewis K. 2015. Persister cells in biofilm associated infections. Adv Exp Med Biol 831:1–9. https://doi.org/10.1007/978-3-319-09782-4_1.
4. Wi YM, Patel R. 2018. Understanding biofilms and novel approaches to the diagnosis, prevention, and treatment of medical device-associated infections. Infect Dis Clin North Am 32:915–929. https://doi.org/10.1016/j.idc.2018.06.009.
5. James GA, Swogger E, Wolcott R, Pulcini E, Secor P, Sestrich J, Costerton JW, Stewart PS. 2008. Biofilms in chronic wounds. Wound Repair Regen 16:37–44. https://doi.org/10.1111/j.1524-475X.2007.00321.x.
6. Murali TS, Kavitha S, Spoorthi J, Bhat DV, Prasad ASB, Upton Z, Ramachandra L, Acharya RV, Satyamoorthy K. 2014. Characteristics of microbial drug resistance and its correlates in chronic diabetic foot ulcer infections. J Med Microbiol 63:1377–1385. https://doi.org/10.1099/jmm.0.076034-0.
7. Bowler PG. 2018. Antibiotic resistance and biofilm tolerance: a combined threat in the treatment of chronic infections. J Wound Care 27:273–277. https://doi.org/10.12968/jowc.2018.27.5.273.
8. Vatan A, Saltoglu N, Yemisen M, Balkan II, Surme S, Demiray T, Mete B, Tabak F, Cerrahpasa Diabetic Foot Study Group. 2018. Association between biofilm and multi/extensive drug resistance in diabetic foot infection. Int J Clin Pract 72:e13060. https://doi.org/10.1111/ijcp.13060.
9. Salisbury AM, Woo K, Sarkar S, Schultz G, Malone M, Mayer DO, Percival SL. 2018. Tolerance of biofilms to antimicrobials and significance to antibiotic resistance in wounds. Surg Technol Int 33:59–66.
10. Bowler PG, Duerden BI, Armstrong DG. 2001. Wound microbiology and associated approaches to wound management. Clin Microbiol Rev 14:244–269. https://doi.org/10.1128/CMR.14.2.244-269.2001.
11. Halstead FD, Lee KC, Kwei J, Dretzke J, Oppenheim BA, Moiemen NS. 2018. A systematic review of quantitative burn wound microbiology in the management of burns patients. Burns 44:39–56. https://doi.org/10.1016/j.burns.2017.06.008.
12. Ortiz Balbuena J, Garcia Madero R, Segovia Gomez T, Cantero Caballero M, Sanchez Romero I, Ramos Martinez A. 2015. Microbiology of pressure and vascular ulcer infections. Rev Esp Geriatr Gerontol 50:5–8. https://doi.org/10.1016/j.regg.2014.08.001.
13. Sahli ZT, Bizri AR, Abu-Sittah GS. 2016. Microbiology and risk factors associated with war-related wound infections in the Middle East. Epidemiol Infect 144:2848–2857. https://doi.org/10.1017/S0950268816000431.
14. Seth AK, Geringer MR, Hong SJ, Leung KP, Galiano RD, Mustoe TA. 2012. Comparative analysis of single-species and polybacterial wound biofilms using a quantitative, in vivo, rabbit ear model. PLoS One 7:e42897. https://doi.org/10.1371/journal.pone.0042897.
15. Wang L, Bassiri M, Najafi R, Najafi K, Yang J, Khosrovi B, Hwong W, Barati E, Belisle B, Celeri C, Robson MC. 2007. Hypochlorous acid as a potential wound care agent: part I. Stabilized hypochlorous acid: a component of the inorganic armamentarium of innate immunity. J Burns Wounds 6:e5.
16. Barrette WC, Jr, Hannum DM, Wheeler WD, Hurst JK. 1989. General mechanism for the bacterial toxicity of hypochlorous acid: abolition of ATP production. Biochemistry 28:9172–9178. https://doi.org/10.1021/bi00449a032.
17. Rani SA, Hoon R, Najafi RR, Khosrovi B, Wang L, Debabov D. 2014. The in vitro antimicrobial activity of wound and skin cleansers at nontoxic concentrations. Adv Skin Wound Care 27:65–69. https://doi.org/10.1097/01.ASW.0000443255.73875.a3.
18. Robson MC, Payne WG, Ko F, Mentis M, Donati G, Shafii SM, Culverhouse S, Wang L, Khosrovi B, Najafi R, Cooper DM, Bassiri M. 2007. Hypochlorous acid as a potential wound care agent: part II. Stabilized hypochlorous acid: its role in decreasing tissue bacterial bioburden and overcoming the inhibition of infection on wound healing. J Burns Wounds 6:e6.
19. Sakarya S, Gunay N, Karakulak M, Ozturk B, Ertugrul B. 2014. Hypochlorous acid: an ideal wound care agent with powerful microbicidal, antibiofilm, and wound healing potency. Wounds 26:342–350.
20. Zmuda HM, Mohamed A, Raval YS, Call DR, Schuetz AN, Patel R, Beyenal H. 2020. Hypochlorous acid-generating electrochemical scaffold eliminates *Candida albicans* biofilms. J Appl Microbiol 129:776–786. https://doi.org/10.1111/jam.14656.
21. Kiamco MM, Zmuda HM, Mohamed A, Call DR, Raval YS, Patel R, Beyenal H. 2019. Hypochlorous-acid-generating electrochemical scaffold for treatment of wound biofilms. Sci Rep 9:2683. https://doi.org/10.1038/s41598-019-38968-y.

22. Livesley NJ, Chow AW. 2002. Infected pressure ulcers in elderly individuals. Clin Infect Dis 35:1390–1396. https://doi.org/10.1086/344059.

23. Braga IA, Pirett CC, Ribas RM, Gontijo Filho PP, Diogo Filho A. 2013. Bacterial colonization of pressure ulcers: assessment of risk for bloodstream infection and impact on patient outcomes. J Hosp Infect 83:314–320. https://doi.org/10.1016/j.jhin.2012.11.008.

24. Braga IA, Brito CS, Filho AD, Filho PP, Ribas RM. 2017. Pressure ulcer as a reservoir of multiresistant Gram-negative bacilli: risk factors for colonization and development of bacteremia. Braz J Infect Dis 21:171–175. https://doi.org/10.1016/j.bjid.2016.11.007.

25. Ramakant P, Verma AK, Misra R, Prasad KN, Chand G, Mishra A, Agarwal G, Agarwal A, Mishra SK. 2011. Changing microbiological profile of pathogenic bacteria in diabetic foot infections: time for a rethink on which empirical therapy to choose? Diabetologia 54:58–64. https://doi.org/10.1007/s00125-010-1893-7.

26. Noor S, Raghav A, Parwez I, Ozair M, Ahmad J. 2018. Molecular and culture based assessment of bacterial pathogens in subjects with diabetic foot ulcer. Diabetes Metab Syndr 12:417–421. https://doi.org/10.1016/j.dsx.2018.03.001.

27. Citron DM, Goldstein EJ, Merriam CV, Lipsky BA, Abramson MA. 2007. Bacteriology of moderate-to-severe diabetic foot infections and in vitro activity of antimicrobial agents. J Clin Microbiol 45:2819–2828. https://doi.org/10.1128/JCM.00551-07.

28. Abbas ZG, Lutale JK, Ilondo MM, Archibald LK. 2012. The utility of Gram stains and culture in the management of limb ulcers in persons with diabetes. Int Wound J 9:677–682. https://doi.org/10.1111/j.1742-481X.2011.00937.x.

29. Brook I, Frazier EH. 1998. Aerobic and anaerobic microbiology of chronic venous ulcers. Int J Dermatol 37:426–428. https://doi.org/10.1046/j.1365-4362.1998.00445.x.

30. Charles PG, Uckay I, Kressmann B, Emonet S, Lipsky BA. 2015. The role of anaerobes in diabetic foot infections. Anaerobe 34:8–13. https://doi.org/10.1016/j.anaerobe.2015.03.009.

31. Choi Y, Banerjee A, McNish S, Couch KS, Torralba MG, Lucas S, Tovchigrechko A, Madupu R, Yooseph S, Nelson KE, Shanmugam VK, Chan AP. 2019. Co-occurrence of anaerobes in human chronic wounds. Microb Ecol 77:808–820. https://doi.org/10.1007/s00248-018-1231-z.

32. Maragakis LL, Perl TM. 2008. *Acinetobacter baumannii*: epidemiology, antimicrobial resistance, and treatment options. Clin Infect Dis 46:1254–1263. https://doi.org/10.1086/529198.

33. Heitkamp RA, Li P, Mende K, Demons ST, Tribble DR, Tyner SD. 2018. Association of *Enterococcus* spp. with severe combat extremity injury, intensive care, and polymicrobial wound infection. Surg Infect 19:95–103. https://doi.org/10.1089/sur.2017.157.

34. Serra R, Grande R, Butrico L, Rossi A, Settimio UF, Caroleo B, Amato B, Gallelli L, de Franciscis S. 2015. Chronic wound infections: the role of *Pseudomonas aeruginosa* and *Staphylococcus aureus*. Expert Rev Anti Infect Ther 13:605–613. https://doi.org/10.1586/14787210.2015.1023291.

35. Jernigan JA, Hatfield KM, Wolford H, Nelson RE, Olubajo B, Reddy SC, McCarthy N, Paul P, McDonald LC, Kallen A, Fiore A, Craig M, Baggs J. 2020. Multidrug-resistant bacterial infections in U.S. hospitalized patients, 2012–2017. N Engl J Med 382:1309–1319. https://doi.org/10.1056/NEJMoa1914433.

36. Barrette WC, Jr, Albrich JM, Hurst JK. 1987. Hypochlorous acid-promoted loss of metabolic energy in *Escherichia coli*. Infect Immun 55:2518–2525. https://doi.org/10.1128/IAI.55.10.2518-2525.1987.

37. da Cruz Nizer WS, Inkovskiy V, Overhage J. 2020. Surviving reactive chlorine stress: responses of Gram-negative bacteria to hypochlorous acid. Microorganisms 8:1220. https://doi.org/10.3390/microorganisms8081220.

38. Fukuzaki S. 2006. Mechanisms of actions of sodium hypochlorite in cleaning and disinfection processes. Biocontrol Sci 11:147–157. https://doi.org/10.4265/bio.11.147.

39. Mai-Prochnow A, Clauson M, Hong J, Murphy AB. 2016. Gram-positive and Gram-negative bacteria differ in their sensitivity to cold plasma. Sci Rep 6:38610. https://doi.org/10.1038/srep38610.

40. Stacy A, McNally L, Darch SE, Brown SP, Whiteley M. 2016. The biogeography of polymicrobial infection. Nat Rev Microbiol 14:93–105. https://doi.org/10.1038/nrmicro.2015.8.

41. Percival SL, Malone M, Mayer D, Salisbury AM, Schultz G. 2018. Role of anaerobes in polymicrobial communities and biofilms complicating diabetic foot ulcers. Int Wound J 15:776–782. https://doi.org/10.1111/iwj.12926.

42. DeLeon S, Clinton A, Fowler H, Everett J, Horswill AR, Rumbaugh KP. 2014. Synergistic interactions of *Pseudomonas aeruginosa* and *Staphylococcus aureus* in an in vitro wound model. Infect Immun 82:4718–4728. https://doi.org/10.1128/IAI.02198-14.

43. Mansito TB, Falcon MA, Moreno J, Carnicero A, Gutierrez-Navarro AM. 1987. Effects of staphylolytic enzymes from *Pseudomonas aeruginosa* on the growth and ultrastructure of *Staphylococcus aureus*. Microbios 49:55–64.

44. Dietrich LE, Price-Whelan A, Petersen A, Whiteley M, Newman DK. 2006. The phenazine pyocyanin is a terminal signalling factor in the quorum sensing network of *Pseudomonas aeruginosa*. Mol Microbiol 61:1308–1321. https://doi.org/10.1111/j.1365-2958.2006.05306.x.

45. Orazi G, Ruoff KL, O'Toole GA. 2019. *Pseudomonas aeruginosa* increases the sensitivity of biofilm-grown *Staphylococcus aureus* to membrane-targeting antiseptics and antibiotics. mBio 10:e01501-19. https://doi.org/10.1128/mBio.01501-19.

46. Renz N, Trebse R, Akgun D, Perka C, Trampuz A. 2019. Enterococcal periprosthetic joint infection: clinical and microbiological findings from an 8-year retrospective cohort study. BMC Infect Dis 19:1083. https://doi.org/10.1186/s12879-019-4691-y.

47. Lagnf AM, Zasowski EJ, Claeys KC, Casapao AM, Rybak MJ. 2016. Comparison of clinical outcomes and risk factors in polymicrobial versus monomicrobial enterococcal bloodstream infections. Am J Infect Control 44:917–921. https://doi.org/10.1016/j.ajic.2016.02.017.

48. Keogh D, Tay WH, Ho YY, Dale JL, Chen S, Umashankar S, Williams RBH, Chen SL, Dunny GM, Kline KA. 2016. Enterococcal metabolite cues facilitate interspecies niche modulation and polymicrobial infection. Cell Host Microbe 20:493–503. https://doi.org/10.1016/j.chom.2016.09.004.

49. Gonzalez S, Fernandez L, Campelo AB, Gutierrez D, Martinez B, Rodriguez A, Garcia P. 2017. The behavior of *Staphylococcus aureus* dual-species biofilms treated with bacteriophage phiIPLA-rodi depends on the accompanying microorganism. Appl Environ Microbiol 83:e02821-16. https://doi.org/10.1128/AEM.02821-16.

50. Iwase T, Uehara Y, Shinji H, Tajima A, Seo H, Takada K, Agata T, Mizunoe Y. 2010. *Staphylococcus epidermidis* Esp inhibits *Staphylococcus aureus* biofilm formation and nasal colonization. Nature 465:346–349. https://doi.org/10.1038/nature09074.

51. Dubin G, Chmiel D, Mak P, Rakwalska M, Rzychon M, Dubin A. 2001. Molecular cloning and biochemical characterisation of proteases from *Staphylococcus epidermidis*. Biol Chem 382:1575–1582. https://doi.org/10.1515/BC.2001.192.

52. Ishihara M, Murakami K, Fukuda K, Nakamura S, Kuwabara M, Hattori H, Fujita M, Kiyosawa T, Yokoe H. 2017. Stability of weakly acidic hypochlorous acid solution with microbicidal activity. Biocontrol Sci 22:223–227. https://doi.org/10.4265/bio.22.223.

53. Mokgatla RM, Gouws PA, Brozel VS. 2002. Mechanisms contributing to hypochlorous acid resistance of a *Salmonella* isolate from a poultry-processing plant. J Appl Microbiol 92:566–573. https://doi.org/10.1046/j.1365-2672.2002.01565.x.

54. Dukan S, Touati D. 1996. Hypochlorous acid stress in *Escherichia coli*: resistance, DNA damage, and comparison with hydrogen peroxide stress. J Bacteriol 178:6145–6150. https://doi.org/10.1128/jb.178.21.6145-6150.1996.

55. Lewandowski Z, Beyenal H. 2013. Fundamentals of biofilm research, 2nd ed. CRC Press, Boca Raton, FL.

56. Renslow R, Donovan C, Shim M, Babauta J, Nannapaneni S, Schenk J, Beyenal H. 2011. Oxygen reduction kinetics on graphite cathodes in sediment microbial fuel cells. Phys Chem Chem Phys 13:21573–21584. https://doi.org/10.1039/c1cp23200b.

57. Christen JA, Parker AE. 2020. Systematic statistical analysis of microbial data from dilution series. JABES 25:339–364. https://doi.org/10.1007/s13253-020-00397-0.

58. Beyenal H, Call DR, Fransson BA, Sultana ST. 2018. Electrochemical reduction or prevention of infections. U.S. patent 20180207301A1, international patent WO/2017/011635.